Towards 3-D Spherical Self-Assembly by Ternary Surfactant Combinations: The Case of Magnetite Nanoparticles

Yanglong Hou,[a,b] Song Gao,*[a] Toshiaki Ohta,[b] and Hiroshi Kondoh[b]

Keywords: Self-assembly / Magnetic properties / Magnetite / Nanoparticles / Super paramagnet

Here we report on a facile one-step route to assemble magnetite nanoparticles into 3D-spherical aggregates with an average diameter of 100 nm. The self-assembly approach was achieved in a solvothermal reduction reaction with a ternary surfactant combination comprising trioctylphosphane oxide (TOPO), polyvinylpyrrolidone (PVP), and oleic acid as the "mortar". Transmission electron microscopy (TEM) investigations indicated that the spherical aggregates were composed of magnetite nanoparticles. The mean size of the individual magnetite particles was estimated to be 6 nm, calculated by the Scherrer equation with the powder X-ray diffraction (XRD) data. The formation mechanism of magnetite spheres can be attributed to the cooperation of the ternary surfactants described above. Magnetic measurements performed by a Quantum Design SQUID magnetometer on the nanoparticles exhibited superparamagnetic behavior above liquid-nitrogen temperatures. Fourier-transform infrared spectroscopy (FTIR), inductively coupled plasma-atomic emission spectrometer (ICP-AE) and X-ray photoelectron spectroscopy (XPS) were also used in the characterization of the assembled magnetite spheres.

Introduction

In recent years, the assembled nanostructures have attracted much interest because of their potential for application in magnetic recording, molecular recognition, biological labeling, and electronic devices.[1−10] The development of simple routes for the fabrication of ordered nanostructures is indispensable for producing new nanodevices. A number of techniques have been exploited in assembly approaches to nanoparticles, such as aerosol-assisted, thiol-modified, DNA-directed, electrostatic-interaction-assisted, and recognition-mediated synthesis.[11−14] The construction of organized metal nanoparticles has recently been a major issue.[15−18] An efficient approach to build self-assembled structures is to harness the spontaneous control of noncovalent interactions between the building blocks, including van der Waals forces,[19,20] π−π interactions,[21] electrostatic forces,[22,23] and hydrogen bonding.[24−26] These molecular interactions are usually constructed through polymer functionalization of nanoscale materials, after which such polymer-functionalized nanoparticles are used as building blocks to fabricate an assembled structure system. For example, Rotello and co-workers reported that monolayer polymer-protected gold nanoparticles self-assembled into spherical aggregates through hydrogen-bonding interactions.[26] The self-assembly of 2-caroxyterthiophene (TTP-COOH) coated Fe_3O_4 aggregates was also achieved by π−π interactions.[21] However, the preparation of ordered nanostructures for applications has been more challenging.

Herein, we report an intriguing finding of self-assembly magnetic particles into spherical aggregates. Our strategy is to use a ternary surfactant combination such as trioctylphosphane oxide (TOPO), polyvinylpyrrolidone (PVP), and oleic acid for the assembly of magnetite nanoparticles. In the presence of these surfactants, the spherical aggregates of magnetite were obtained by a solvothermal reduction of iron(III) acetylacetonate with hydrazine in ethylene glycol. Note that the spherical aggregates of magnetite nanoparticles formed spontaneously without any external force.

Results and Discussion

Powder XRD and TEM measurements were employed to study the structure and the morphology of the obtained products. The XRD pattern of the sample (Figure 1) reveals the characteristic diffraction peaks of magnetite (JCPDS file, 19−629). The broad nature of the peaks results from nanosized magnetite aggregates. The average size of the individual magnetite particles is about 6 nm, calculated by the

[a] State Key Laboratory of Rare Earths Materials Chemistry and Applications, College of Chemistry and Molecular Engineering, Peking University,
Beijing 100871, P. R. China
Fax: (internat.) +86-10-6275-1708
E-mail: gaosong@pku.edu.cn
[b] Department of Chemistry, School of Science, The University of Tokyo,
Tokyo 113-0033, Japan
Supporting information for this article is available on the WWW under http://www.eurjic.org or from the author.

Scherrer equation.[27] In addition, far-IR and XPS spectra were applied to confirm the formation of magnetite rather than hematite. The far-FTIR spectrum of the sample is in good agreement with that of commercially available magnetite powder (Alfa catalog No 44120, see Supporting Information Figure S1), suggesting the formation of magnetite. Furthermore, as shown in the XPS spectra (Figure S2, see Supporting Information), the binding energy of Fe $2p_{3/2}$ is 711.4 eV, which is very close to that of magnetite. TEM images (Figure 2) show that the mean size of the spherical aggregates is about 100 nm. The selected-area electron diffraction (SAED) pattern of the sample indicates the crystalline characteristics of magnetite aggregates (see c in Figure 2). The formation process of assembled magnetite aggregates is illustrated in Scheme 1. It is well-known that the dipole−dipole interaction between magnetic nanoparticles strongly affects their shape and properties. However, this magnetic interaction scarcely contributes to the formation of spherical nanostructures of magnetite nanoparticles; similar behavior has also been observed in the TTP-COOH-coated Fe_3O_4 nanoparticle system.[21] In the present system, the key factor that directs the assembly of spheres is considered to be the combination of ternary surfactants on the surface of the magnetite nanoparticles, although the interaction between magnetite nanoparticles and surfactants is not fully understood. When only PVP was used in the reaction, iron nanoparticles (ca. 60 nm) without spherical aggregation were obtained,[28] whereas the similar systems with PVP and oleic acid produced magnetite nanoparticles where the size could be controlled.[29,30] It was supposed that the process to produce assembled spherical nanostructures was controlled by the diffusion growth,[31] that is, a number of nanoparticles aggregated around a single nanoparticle automatically forming spherical aggregates, which have the lowest surface energy. As the reaction progresses, magnetite nanoparticles coated with surfactants were initially produced. This is followed by the assembly of the individual surfactant-coated magnetite nanoparticles into spherical structures with the help of intermolecular interactions, which result from the cooperation of TOPO, oleic acid, and PVP.[31,32] The total content of the surfactants was 54.4 wt-%, estimated by ICP measurements. As shown in the FTIR pattern (Figure S3, see Supporting Information), the characteristic peak of PVP in the sample ($\tilde{\nu}$ = 3398 cm^{-1}) has a small blue-shift, relative to that of neat

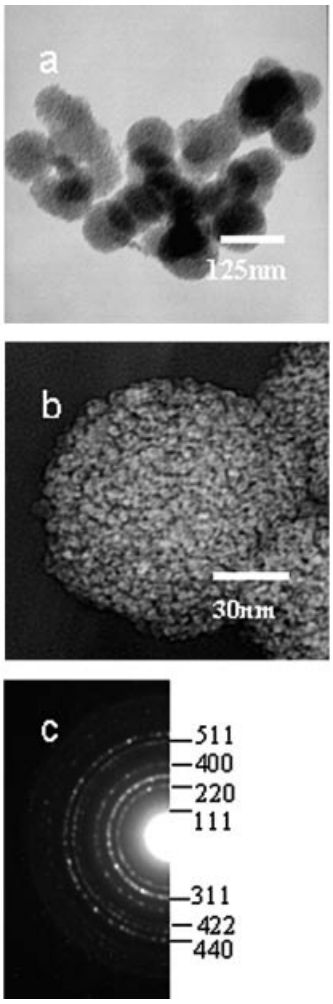

Figure 2. TEM images of (a) self-assembled spherical aggregates, (b) an enlarged image of a individual sphere, and (c) the selected-area electron diffraction pattern of the sample

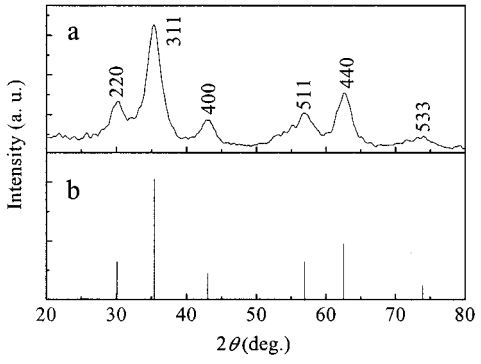

Figure 1. XRD patterns of the sample (a) and commercial magnetite powder (b) with JCPDS No. 19-629

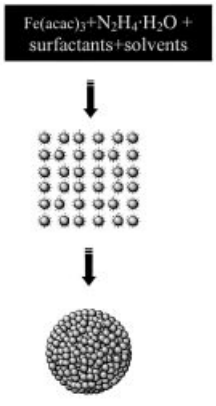

Scheme 1. Schematic pattern of self-assembly of 3D magnetic spheres

PVP, while the peak intensities of TOPO and oleic acid are obviously weakened, which is most likely ascribed to the interaction of the surfactants with the nanoparticles. This result also confirms the above description on the formation process of nanoparticle aggregates. Further studies are required to characterize the structural features and the interaction between the nanoparticles and the surfactants in the assembled magnetite aggregates.

The magnetization curves were measured as a function of temperature with an applied field of 100 Oe between 5 and 300 K using field-cooling (FC) and zero-field-cooling (ZFC) procedures. When the sample is cooled to the zero magnetic field temperature, the total magnetization of the particles will be zero since the magnetic moments of individual particles are randomly oriented. An external magnetic field energetically favors the reorientation of the moments of the individual particles along the applied field at low temperatures. As the temperature increases, more and more particles reorient their magnetization with the external field and the total magnetization increases, and reaches the maximum at the blocking temperature (T_B = 70 K), shown in Figure 3. At this temperature, the thermal energy becomes similar to the energy gained by aligning the particle magnetic vectors in the weak field; the transition from ferromagnetic to superparamagnetic behavior is observed. At temperatures higher than T_B, one can see that the magnetization decreases and follows a Curie−Weiss law corresponding to the superparamagnetic behavior, also suggesting the absence of strong dipole−dipole interactions. Such behavior has been reported for several particle systems, in agreement with theoretical predictions.[33] In the case of field cooling, magnetization monotonously increases as the temperature decreases. Below T_B, the field-cooling curve splits from the zero-field-cooling curve.

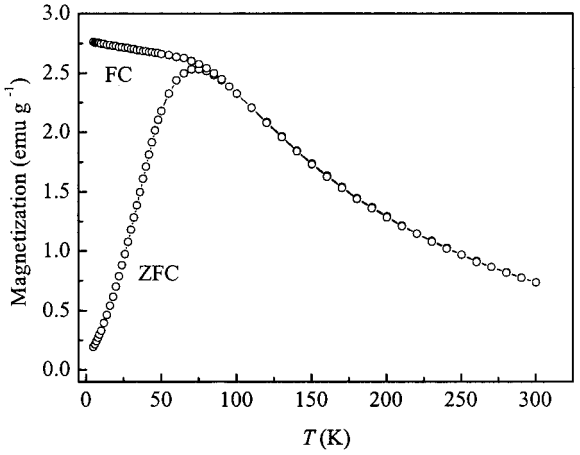

Figure 3. ZFC and FC curves of self-assembled magnetite spherical aggregates measured with a field of 100 Oe

The divergence of magnetization below T_B in ZFC-FC procedures is attributed to the existence of the magnetic anisotropy barriers. The derivative of the magnetization decay plot, $f(T)$ represents the distribution of anisotropy energy barriers.[34]

$$f(T) = \frac{d}{dT}\left(\frac{M_{ZFC}}{M_{FC}}\right) \quad (1)$$

This is represented by Equation (1) where M_{ZFC} denotes only the contribution of nanoparticles, for which the energy barriers are overcome by the thermal energy at the measurement; while M_{FC} represents the contribution of all the nanoparticles. The calculated magnetic anisotropy distribution of 6 nm spherical Fe_3O_4 aggregates is shown in Figure 4 and fitted by the Gauss function. The center and width values are 33.0 K and 40.7 K, respectively. The narrow distribution indicates that the nanoparticles have a uniform size. For superparamagnetic particles, $T_B = KV/25k$, where T_B is the blocking temperature, K denotes the magnetic anisotropy constant, k the Boltzmann's constant, and V the volume of the particles; below T_B the free movement ($\mu_p = Ms \cdot V$) is blocked by the anisotropy, where Ms represents the saturation magnetization. Above T_B, kT activates the magnetic moment so that the system appears to have the characteristics of a superparamagnet. The anisotropy constant can be estimated by referring to the experimental data of the blocking temperature. In the present system, the anisotropy constant of the assembled magnetite nanoparticle with a size of 6 nm is 2.14×10^6 erg·cm^{-3}.

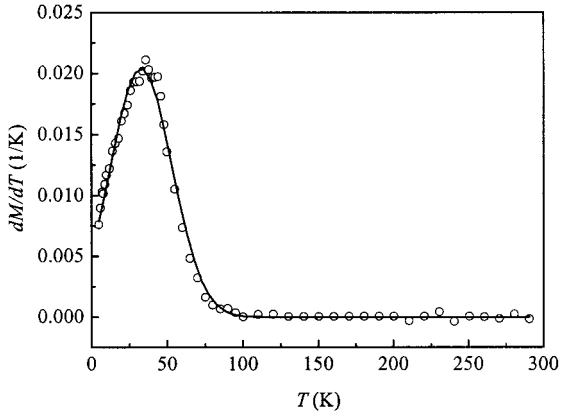

Figure 4. The energy barrier distribution of magnetic anisotropy in the self-assembled magnetite aggregates

A representative hysteresis loop of assembled Fe_3O_4 spheres is shown in Figure 5. At 300 K, the saturation magnetization of the assembled Fe_3O_4 particles is 83 emu/g at 30 kOe, while that of the commercial magnetic liquid is 123 emu/g(Fe).[35] The decrease of the saturation magnetization is most likely attributed to the existence of surfactants on the surface of the Fe_3O_4 nanoparticles. Some studies suggested that the noncollinear spin structure, which originated from pinning the surface spins and coated surfactants to the iron oxide interface, results in the reduction of the magnetic moment in such nanoparticles.[36] The coercive force of self-assembled spheres is 292 Oe at 5 K (as shown

by the inset in Figure 5), while the coercivity at room temperature is almost negligible, which is a characteristic of superparamagnetic materials.[37,38]

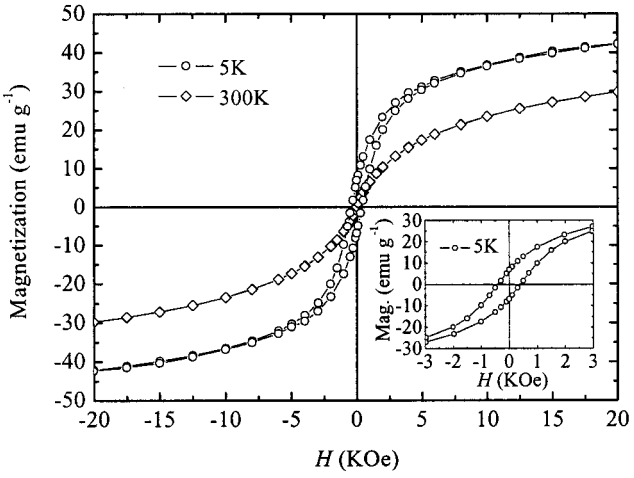

Figure 5. Magnetization of self-assembled magnetite aggregates as a function of the applied field measured at 5 K and 300 K. The inset is an enlarged magnetization curve of self-assembled Fe_3O_4 nanoparticles at 5 K

Conclusion

In this work, a facile and effective route has been developed to build 3D, spherical aggregates of nanoparticles with ternary surfactants as the "mortar". The results reveal that the self-assembly strategy is an efficient way to create novel nanostructured systems. The magnetic behavior of spherical magnetite aggregates shows superparamagnetic characteristics above liquid-nitrogen temperatures. The magnetic anisotropy distribution of the spherical magnetite aggregates has also been deduced from magnetic data.

Experimental Section

General: The synthesis and assembly of magnetite spheres was performed by a one-step procedure, in which $Fe(acac)_3$ (acac = acetylacetonate) was partially reduced by a mixture of hydrazine and ethylene glycol and spontaneously assembled into spherical nanostructures in the presence of a combination of surfactants including TOPO, PVP, and oleic acid. In a typical procedure, a solution of 70 mL was first prepared by dissolving $Fe(acac)_3$ (0.2 g), TOPO (99 %, 0.2 g), PVP (M_r = 55,000, 0.2 g), and oleic acid (0.1 mL) in ethylene glycol, after which 10 % $N_2H_4{\cdot}H_2O$ (2 mL) was added. The mixture was transferred into an autoclave and heated to 180 °C for 12 h and then allowed to cool to room temperature. The black products deposited onto the bottom of the autoclave indicated the formation of magnetite. The final product was collected and washed with methanol/$CHCl_3$ (1:1) and distilled water to remove possible excess surfactants, $N_2H_4{\cdot}H_2O$, and by-products. The black product was then dried in vacuo at 60 °C for 12 h. Powder XRD patterns of the sample were obtained on a Rigaku Dmax/2000 diffractometer with Cu-K_α radiation. TEM images to determine the size and morphology of the product were collected with a HITACHI H-800 electron microscope (200 kV). IR spectra (KBr pellets) were recorded on a NICOLET Magna-IR 750 spectrophotometer. X-ray photoelectron spectroscopy (XPS) data were collected on a ESCA-lab5. The content of magnetite in the product was determined on an inductively coupled plasma-atomic emission spectrometer (ICP). Magnetic studies were carried out by using a Quantum Design SQUID magnetometer.

Acknowledgments

Financial support from the National Science Fund for Distinguished Young Scholars (20125104), NFSC no.20221101, and the Chinese Postdoctoral Research Fund are gratefully acknowledged.

[1] M. Bruchez, M. Moronne, P. Gin, S. Weiss, A. P. Alivisatos, *Science* **1998**, *281*, 2013−2016.
[2] C. B. Murray, S. Sun, H. Doyle, T. Betley, *MRS. Bull.* **2001**, 985−989.
[3] J. Z. Zhang, Z. L. Wang, J. Jiu, S. Chen, G. Y. Liu. *Self-assembled Nanostructures*, Kluwer, New York, **2003**.
[4] S. Sun, C. B. Murray, D. Weller, L. Folks, A. Moser, *Science* **2000**, *287*, 1989−1992.
[5] M. Green, P. O'Brien, *Chem. Commun.* **2001**, 1912−1913.
[6] E. V. Shevchenko, D. Talapin, A. L. Rogach, A. Kornowski, M. Haase, H. Weller, *J. Am. Chem. Soc.* **2001**, *124*, 11480−11485.
[7] F. Dumestre, B. Chaudret, C. Amiens, M. C. Fromen, M. J. Casanove, P. Renaud, P. Zurcher, *Angew. Chem. Int. Ed.* **2002**, *41*, 4286−4289.
[8] H. Bönnemann, R. M. Richards, *Eur. J. Inorg. Chem.* **2001**, 2455−2480.
[9] G. Schmid, N. Beyer, *Eur. J. Inorg. Chem.* **2002**, 835−837.
[10] J. S. Bradley, B. Tesche, W. Busser, M. Maase, M. T. Reetz, *J. Am. Chem. Soc.* **2000**, *122*, 4631−4636.
[11] Y. Lu, H. Fan, A. Stump, T. L. Ward, T. Rieker, C. J. Brinker, *Nature* **1999**, *398*, 223−226.
[12] L. Motte, M. P. Pileni, *Appl. Surf. Sci.* **2000**, *164*, 60−67.
[13] R. C Mucic, J. J. Storhoff, C. A. Mirkin, R. L. Letsinger, *J. Am. Chem. Soc.* **1998**, *120*, 12674−12675.
[14] B. L. Frankamp, O. Uzun, F. Iihan, A. K. Boal, V. M. Rotello, *J. Am. Chem. Soc.* **2002**, *124*, 15146−15147.
[15] A. P. Alivisatos, K. P. Johnsson, X. Peng, T. E. Wilson, C. J. Loweth, M. P. Bruchez Jr., P. G. Schultz, *Nature* **1996**, *382*, 609−611.
[16] X. Peng, L. Manna, W. Yang, J. Wickham, E. Scher, A. Kadavanich, A. P. Alivisatos, *Nature* **2000**, *404*, 59−61.
[17] K. Naka, H. Itoh, Y. Chujo, *Langmuir* **2003**, *19*, 5496−5501.
[18] L. E. Euliss, S. G. Grancharov, S. O'Brien, T. J. Deming, G. D. Stucky, C. B. Murray, G. A. Held, *Nano Lett.* **2003**, *3*, 1489−1493.
[19] J.-M. Lehn, *Supramolecular chemistry*, VCH, Weinheim, **1995**.
[20] R. P. Andres, J. D. Bielefeld, J. I. Henderson, D. B. Janes, V. R. Kolagunta, C. P. Kubiak, W. J. Mahiney, R. G. Osifchin, *Science* **1996**, *273*, 1690−1694.
[21] J. Jin, T. Iyoda, C. Cao, Y. Song, L. Jiang, T. J. Li, D. B. Zhu, *Angew. Chem. Int. Ed.* **2001**, *40*, 2135−2138.
[22] M. C. T. Fyfe, J. F. Stoddart, *ACC. Chem. Res.* **1997**, *30*, 393−401.
[23] F. Caruso, R. Caruso, H. Mohwald, *Science* **1998**, *282*, 1111−1114.
[24] C. A. Mirkin, R. L. Letsinger, R. C. Mucic, J. J. Storhoff, *Nature* **1996**, *382*, 607−609.
[25] J. Rebek, *Acc. Chem. Res.* **1999**, *32*, 278−286.
[26] A. K. Boal, F. Ilhan, J. E. Derouchey, T. Thurn-Albercht, T. P. Russell, V. M. Rottello, *Nature* **2000**, *404*, 746−748.
[27] H. P. Klug, L. E. Alexander, *X-ray Diffraction Procedures for polycrystalline and Amorphous Materials*; John Wiley & Sons, New York, **1962**, pp. 491−538.

[28] Y. L. Hou, S. Gao, *J. Alloy Com.* **2004**, *365*, 112−116.
[29] S. Sun, H. Zeng, *J. Am. Chem. Soc.* **2002**, *124*, 8204−8205.
[30] Y. Hou, J. Yu, S. Gao, *J. Mater. Chem.* **2003**, *13*, 1983−1987.
[31] D. V. Goia, E. Matijevi, *New J. Chem.* **1998**, 1203−1215.
[32] X. Peng, J. Wickham, A. P. Alivisatos, *J. Am. Chem. Soc.* **1998**, *120*, 5343−5344.
[33] E. del Barco, J. Asenjo, X. X. Zhang, R. Pieczynski, A. Julià, J. Tejada, R. F. Ziolo, *Chem. Mater.* **2001**, *13*, 1487−1490.
[34] A. J. Rondinone, A. C. S. Samia, Z. J. Zhang, *J. Phys. Chem. B* **1999**, *103*, 6876−6880.
[35] K. S. Suslick, M. Fang, T. Hyeon, *J. Am. Chem. Soc.* **1996**, *118*, 11960−11961.
[36] R. H. Kodama, A. E. Berkowitz, E. J. McNiff, S. Foner, *Phys. Rev. Lett.* **1996**, *77*, 394−397.
[37] I. Prigogine, S. A. Rice, *Advances in Chemical Physics*, John Wiley & Sons, New York, **1997**, vol. 98.
[38] *Nanoscale materials in Chemistry:* Kenneth J. Klabunde (Ed.), John Wiley & Sons, New York, **2001**, 205.

Received October 24, 2003

